

Superconducting properties of Nb-CuMn multilayers

C. Attanasio, L. Maritato, S. L. Prischepa,^{a)} and M. Salvato
Dipartimento di Fisica, Università degli Studi di Salerno, Baronissi (Sa), I-84081, Italy

B. N. Engel and C. M. Falco
Department of Physics, Optical Sciences Center and Arizona Research Laboratories, University of Arizona, Tucson, Arizona 85721

(Received 7 February 1994; accepted for publication 14 November 1994)

The superconducting properties of spin-glass superconducting multilayers made of Nb (superconducting) and CuMn (spin glass) have been studied. The superconducting critical temperature T_c of the multilayers was strongly dependent on the thickness of the spin-glass layers. The Radovic *et al.* theory [Phys. Rev. B **44**, 759 (1991)], which foresees a phase difference $0 \leq \phi \leq \pi$ between neighboring superconducting layers, has given a qualitative description of these experimental data. The parallel and perpendicular critical magnetic-field measurements have shown many interesting effects related to the reduced dimensionality of the samples. © 1995 American Institute of Physics.

I. INTRODUCTION

The coexistence between superconductivity and magnetism has been an intriguing issue of study both for its practical and fundamental consequences. Heavy fermions,¹ Chevrel phase compounds,² and rare-earth rhodium-borides³ are examples of materials that show interesting physical properties due to the interplay of superconducting and magnetic effects. While antiferromagnetic order truly coexists with superconductivity below the Néel temperature,⁴ ferromagnetic order below the Curie temperature generally destroys Copper pairs, resulting, as in the case of ErRh_4B_4 ,⁵ in reentrant superconductivity. A new class of materials, such as $(\text{Nd}_{1-x}\text{Th}_x)\text{Ru}_2$,⁶ has also displayed, in a certain range of composition, multiple reentrant transitions between the normal and the superconducting state due to interaction with a spin-glass order. Finally, in some high- T_c compounds such as $\text{YBa}(\text{CuFe})\text{O}$,⁷ coexistence of superconductivity with a spin-glass magnetic order has been observed by neutron-diffraction analysis.

The realization of artificial multilayers with magnetic and superconducting phases gives the opportunity of studying the interplay in different situations by suitably choosing both the materials and the relative thicknesses.⁸ Moreover, multilayers of superconducting materials have recently been used⁹ as test systems to check some effects observed on high critical temperature oxides, in order to discriminate if they were related to intrinsic properties of these new compounds or to the reduced dimensionality present in layered superconductors.

In the present work we designed our multilayers to obtain superconductivity in the presence of spin-glass order and to study the effects of reduced dimensionality in a system with superconductor-normal-superconductor (SNS) coupling in the presence of magnetic impurities.

We chose Nb as superconducting material and CuMn with two different Mn concentrations (7% and 14%) as spin

glass. The choice of Nb was related to its highest critical temperature, 9.2 K, among the superconducting elements, while that of CuMn was related to its well-known properties of metallic spin glass^{10,11} and to the numerous works already present in literature about CuMn-based and Nb-Cu multilayers.¹²⁻¹⁴ In all our multilayers we kept the Nb layer thickness fixed (~ 230 Å) while varying the CuMn layer thickness in the range 3–50 Å.

The measured superconducting properties of the system were strongly influenced by the presence of CuMn layers. The reduced dimensionality of the system also played an important role in the temperature behavior of the critical magnetic field and showed similar effects to those observed in the resistive transition curves of high- T_c materials in the presence of an externally applied magnetic field.

II. EXPERIMENT

A. Sample preparation and experimental techniques

The multilayers were deposited on sapphire substrates using magnetically enhanced dc triode sputtering with a rotating substrate holder alternately passing over the targets.¹⁵

The composition of the magnetic phase was determined by Rutherford backscattering (RBS) analysis which was also used to calibrate the sputtering rates. The exact composition of the CuMn was $\text{Cu}(9.44)\text{Mn}(6.6)$ for the lower Mn concentration and $\text{Cu}(85.6)\text{Mn}(14.4)$ for the higher.

A series of Nb-Cu multilayers with Cu thicknesses in the range 4–50 Å was also realized to compare the properties in the magnetic and nonmagnetic case. The layer periodicity was confirmed by small-angle x-ray analysis. All the samples prepared were made of 10 bilayers with a total thickness varying from ~ 2250 to ~ 2600 Å. The first deposited layer was always CuMn or Cu while the top layer was made of Nb.

All the temperature measurements were made using a sample holder with a Copper block in which the sample was held in close thermal contact with a Ge-doped thermometer suitably designed for magnetic measurements. A superconducting solenoid with high uniformity of the field in the zone

^{a)}Permanent address: Radioengineering Institute, P. Brovka str. 6, 220600, Minsk, Byelorussia, CIS.

TABLE I. Characteristics of the sample studied. For each sample we report the thickness of the niobium and of the normal layer (Cu or CuMn), the percentage of Mn, the critical temperature, the room-temperature electrical resistivity, the β ratio, and the electronic diffusion coefficient. M/m is the anisotropic Ginzburg–Landau mass ratio.

Sample	d_{Nb} (Å)	d_{N} (Å)	% Mn	T_c (K)	$\rho_{300\text{ K}}$ ($\mu\Omega$ cm)	$\beta_{10\text{ K}} = \rho_{300\text{ K}}/\rho_{10\text{ K}}$	D (cm^2/s)	M/m
NC8	237	7.7	...	8.15	26.35	2.35	1.80	...
NCMA3	232	3.0	14.4	7.23	28.13	2.17	1.76	3.7
NCMA4	232	4.0	14.4	7.08	28.25	2.24	1.77	2.8
NCMA6	232	5.9	14.4	7.00	22.57	2.76	1.90	2.9
NCMA8	232	7.9	14.4	5.91	28.48	2.21	2.34	6.0
NCMA16	232	15.9	14.4	4.57	29.92	2.25	2.66	15.7
NCMA32	232	31.8	14.4	4.67	28.62	2.09	2.58	30.3
NCMA50	232	49.8	14.4	4.79	28.34	2.15	2.38	36.0
NCM4	232	4.7	6.6	7.61	25.41	2.4	1.76	...
NCM6	232	7.1	6.6	7.30	26.49	2.32	2.01	...
NCM8	232	9.4	6.6	6.90	25.04	2.46	2.12	3.8
NCM16	232	18.8	6.6	5.92	27.23	2.45	2.17	...
NCM32	232	37.7	6.6	5.81	22.72	2.32

where the samples were situated was used for the critical magnetic-field measurements. The experimental setup allowed measurements in the temperature range 2–300 K with externally applied magnetic fields up to 2 T.

In Table I we have summarized some of the main properties of the fabricated multilayers.

B. Sample characterization: Results and discussion

1. Electrical measurements

We measured the electrical resistivity of our samples using a four-contact Van de Pauw technique. The values obtained at room temperature and at 10 K are shown in Figs. 1(a) and 1(b). They are practically independent of the layering and in the range 20–30 $\mu\Omega$ cm at room temperature and between 10 and 15 $\mu\Omega$ cm at 10 K. Assuming a parallel resistor model,¹⁶ we have for our multilayers a resistivity ρ given by

$$\rho = \frac{\rho_s \rho_n}{f_n \rho_s + f_s \rho_n}, \quad (1)$$

where ρ_s is the resistivity of the Nb layers, ρ_n is the resistivity of the CuMn (or Cu) and f_s and f_n are, respectively, the relative amounts of Nb and CuMn (or Cu) present in the system. Obviously $f_s + f_n = 1$. Using for ρ_s and ρ_n at 10 K values close to those measured in previous works^{13,17} (respectively, $\rho_s \sim 10 \mu\Omega$ cm and $\rho_n \sim 19 \mu\Omega$ cm) we get from Eq. (1) resistivity values in good agreement with the low-temperature experimental data.

The values obtained in the Nb-Cu series are in the same range. This could be surprising assuming a Cu resistivity close to the bulk value but can be understood considering that the electronic mean free path of Cu is strongly reduced by the layering.^{13,16}

2. Critical temperature measurements

In Fig. 2 the resistively measured superconducting critical temperatures, T_c versus the nonsuperconducting layer thickness d_n , are shown for the samples of the three series

[Nb-Cu(93)Mn(7), Nb-Cu(86)Mn(14), Nb-Cu]. As can be seen, the behavior versus the thickness of the normal layers, d_n , is significantly different when going from the nonmagnetic case (Nb-Cu) to the magnetic case (Nb-CuMn). The decrease in T_c with the increase of d_n is stronger in the series with Cu(86)Mn(14). In the case of the Nb-Cu series the solid line obtained from the de Gennes–Werthamer theory,¹⁸ using

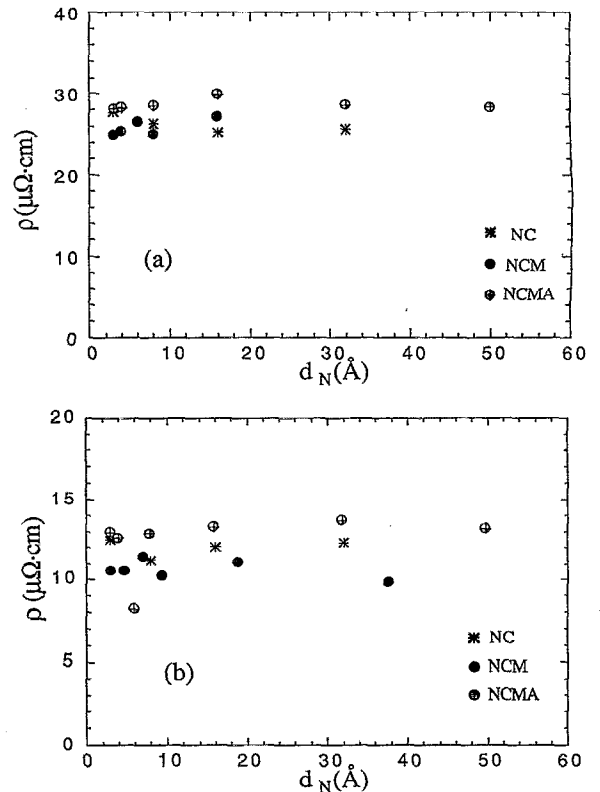


FIG. 1. (a) Room-temperature electrical resistivity vs CuMn (or Cu) layer thickness and (b) electrical resistivity vs CuMn (or Cu) layer thickness at $T=10$ K for our samples: (★) NbCu (NC); (●) NbCu(93)Mn(7)(NCM); and (⊕) NbCu(86)Mn(14)(NCMA) multilayers.

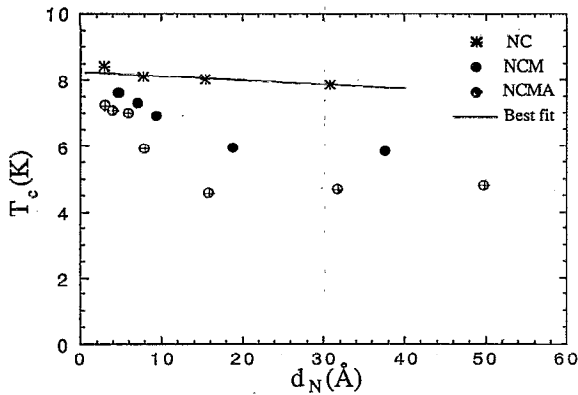


FIG. 2. Superconducting critical temperature vs CuMn (or Cu) layer thickness. Symbols are the same as in Fig. 1. The solid line is obtained by using the de Gennes–Werthamer theory, using $\rho_s=10.8 \mu\Omega \text{ cm}$, $\rho_n=18.8 \mu\Omega \text{ cm}$, and $T_c=8.28 \text{ K}$.

$\rho_s=10.8 \mu\Omega \text{ cm}$, $\rho_n=18.8 \mu\Omega \text{ cm}$, and $T_c=8.28 \text{ K}$, describes the experimental data with good agreement.

The same is not true for the T_c behavior of the other two series. For these data the Hauser, Theurer, and Werthamer theory,^{19,20} developed in the case of a pair-breaking mechanism related to both the proximity effect and to the presence of randomly distributed magnetic impurities in the normal layers, does not describe at all the observed behavior. We would like to point out, in particular, that for values of the normal layer thickness larger than 40 \AA , we observed a non-monotonic behavior of T_c which is not foreseen in the Hauser and co-workers theory.

Similar experimental data have been observed in the case of V/Fe multilayers,²¹ and have been explained using the Bulaevkii, Kuzii, and Sobyenin π -phase theory²² applied to the case of magnetic layered superconductors by Radovic *et al.*²³

The dashed line in Fig. 3 is the best-fit curve to the critical temperature measurements, reported as a function of

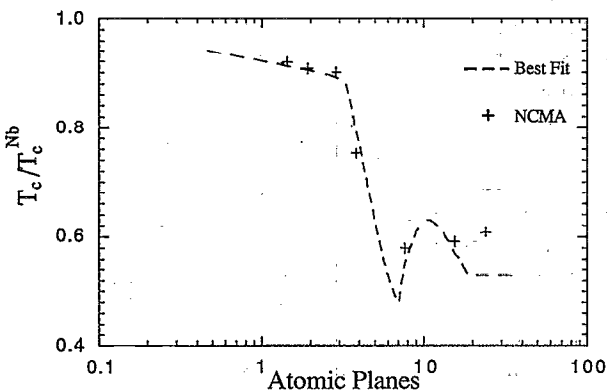


FIG. 3. Reduced superconducting critical temperature (normalized with respect to the Nb single-layer value) vs the number of atomic planes for the NbCu(86)Mn(14) multilayers. The dashed line is calculated by using the Radovic *et al.* theory by putting $d_s/\xi_s=4.4$ and $\Theta_D/T_c=35$. We obtain $\epsilon=6$ as a fitting parameter.

the number of the CuMn atomic planes, for the Nb-Cu(86)Mn(14) series, obtained using the Radovic *et al.* theory,²³ in which the superconducting order parameter is allowed to have phase difference in the range $0 \leq \phi \leq \pi$ when going from one superconducting layer to another. In passing we want to say that even though our samples were all asymmetric (in contrast to the case analyzed in Ref. 23), this should not completely invalidate a comparison to the Radovic *et al.* theory. The best-fit curve is obtained by fixing, as input parameters, $d_s/\xi_s=4.4$ and $\Theta_D/T_c=35$ for our Nb, and by using as a fitting parameter $\epsilon=6$, with ϵ being in the Radovic *et al.* theory a measure of the influence of the magnetic layers on the critical temperature T_c of the entire sample. The distance between the atomic planes of the CuMn has been taken equal to that of the Cu (2.08 \AA) and ξ_M , the characteristic penetration length of Cooper pairs in normal layers, was assumed equal to ten atomic planes. The value for ξ_s has been deduced by measuring the electronic diffusion constant (see following section) and the critical temperature T_c of a single Nb film of 230 \AA , by means of the relation $\xi_s^2 = \hbar D / 2 \pi k_B T_c$.

As is clearly seen the comparison gives only a qualitative agreement, but some considerations can be inferred from these data. The value $\epsilon=6$ indicates, in fact, a very weak magnetic strength of the CuMn layers (in comparison to the value $\epsilon=2$ used to fit the data of the strong magnetic V/Fe multilayers in Ref. 21).

Moreover, the theory is able to explain the quite fast decrease of the critical temperatures in the range of 10–50 atomic planes not explained by the Hauser and co-workers theory. On the other hand there is only some qualitative indication of the nonmonotonicity in the T_c versus atomic planes curve.

Probably, it could be argued that in the presence of a spin-glass order a pair breaking parameter which takes into account the peculiarity of this magnetic system should be used. Stephan and Carbotte²⁴ suggested for a spin-glass superconducting system a temperature-dependent pair breaking parameter α given by

$$\alpha(T) = \frac{nm p_F J^2}{2 \pi^2 \hbar^3} [T \chi(T) + Q(T)]. \quad (2)$$

Here n is the concentration of magnetic atoms, m is the electronic mass, p_F is the Fermi momentum, J is the exchange integral, $\chi(T)$ is the magnetic susceptibility, and $Q(T)$ is the spin-glass-order parameter proportional to $(1 - T/T_f)$, where T_f is the spin-glass freezing temperature. Preliminary measurements of the magnetic susceptibility, using a superconducting quantum interference device magnetometer, have indicated a hysteretic behavior with temperature of the zero-field and field cooled magnetization curves when the external field is applied parallel to the plane of the films. More experimental work to check the validity of this model is in progress.

3. Magnetic measurements

Due to the anisotropic nature of our samples we will separate this subsection in two subsections *a* and *b* dedi-

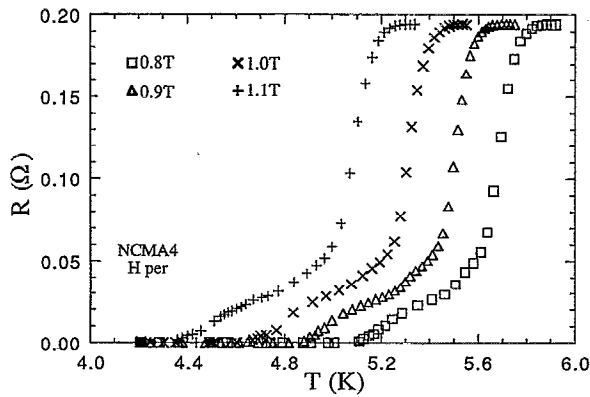


FIG. 4. Resistive transition curves of the sample with 4 Å of Cu(86)Mn(14) at different values of externally applied perpendicular magnetic fields.

ated, respectively, to the measurements in the direction perpendicular and parallel to the plane of the films.

a. Perpendicular magnetic measurements. The transition curves at different values of the externally applied magnetic field are shown in Fig. 4 for a sample with 4 Å of Cu(86)Mn(14). It is easily seen that the onset critical temperatures (the temperatures at which the normal resistance drops by 10% of its value) decrease with the increasing field, while the shape of the curves does not change at least in the higher-temperature part. With increasing magnetic fields the lower-temperature part of the transition curves develops a tail as has been also observed in the case of high- T_c oxides.²⁵ We extensively discuss this effect later.

In Fig. 5 we show the $H_{c2\perp}$ vs T curves for the series with Cu(86)Mn(14). In all the samples the $H_{c2\perp}$ temperature behavior is linear as expected for an anisotropic superconductor, in which $H_{c2\perp}$ is given by²⁶

$$H_{c2\perp} = \frac{\phi_0}{2\pi\xi_{\parallel}^2(T)}, \quad (3)$$

where ϕ_0 is the flux quantum and $\xi_{\parallel}(T)$ is the anisotropic superconducting coherence length in the direction parallel to

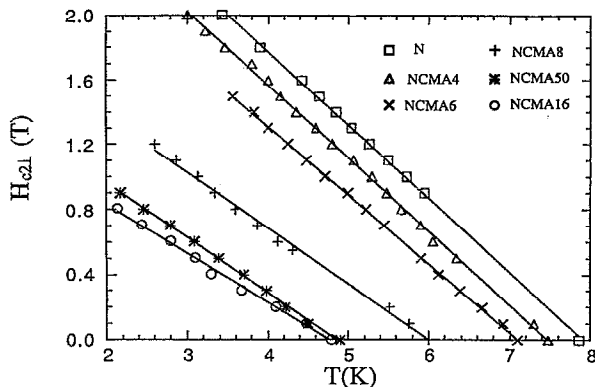


FIG. 5. Perpendicular critical magnetic fields as a function of temperature for different samples. Solid lines represent the best linear fits. N refers to the single Nb film of 230 Å.

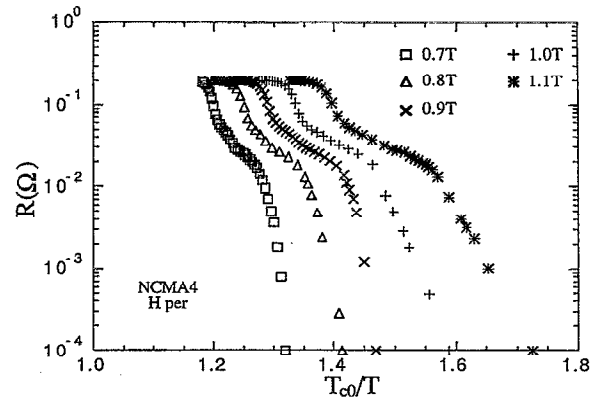


FIG. 6. Arrhenius plot of the $R(T)$ of the sample of Fig. 4 for different values of perpendicular magnetic field.

the plane of the film. We did not observe any appreciable deviation from the linear behavior of these curves, as should be in the case of the presence of a magnetic ordering starting at temperatures lower than T_c . Moreover, in the dirty superconducting limit we can write

$$\left(\frac{dH_{c2\perp}}{dT}\right)_{T=T_c} = \frac{-ck_B}{1.08eD}, \quad (4)$$

where k_B is the Boltzmann constant and D is the electronic diffusion coefficient of the multilayer, defined as $D = v_F l / 3$, with v_F being the Fermi velocity and l the electronic mean free path.²⁷ From the measured data we obtained D values increasing with increasing CuMn layer thicknesses up to 16 Å and decreasing for larger thicknesses. We point out that our D values took into account the transport properties of each component material and the electron scattering at the interfaces between layers. It is then worth mentioning that in the limit of decoupled layers (larger CuMn thicknesses) the measured D values tended toward the value $D = 1.76 \text{ cm}^2/\text{s}$ measured for the electronic diffusion constant in the case of a single Nb film of 230 Å.

Interesting results were also obtained by the analysis of the resistance tails present in the lower part of the transition curves. In Fig. 6 we have replotted the data of Fig. 4 in Arrhenius fashion. In each curve is then clearly visible a sharp downward kink at a field-dependent temperature $T^*(H)$. The presence of such kinks was observed for CuMn thicknesses up to 16 Å. Starting from $d_{\text{CuMn}} = 32 \text{ Å}$, the downward kink disappeared. As an example, in Fig. 7 we have shown the Arrhenius plots of the transition curves for the sample with 50 Å of Cu(86)Mn(14) in the presence of perpendicular magnetic fields up to about 1 T. The absence of any kinks is evident. Similar results, with no kinks, were obtained in the case of parallel external magnetic fields for all the CuMn thicknesses, in the case of a single Nb film of 230 Å and in the case of nonmagnetic Nb-Cu multilayers with Cu thicknesses up to 10 Å.

The same kinds of Arrhenius plots were obtained for high- T_c oxides and MoGe/Ge multilayers.^{9,25} In this last case, the authors observed that above T^* the resistance of

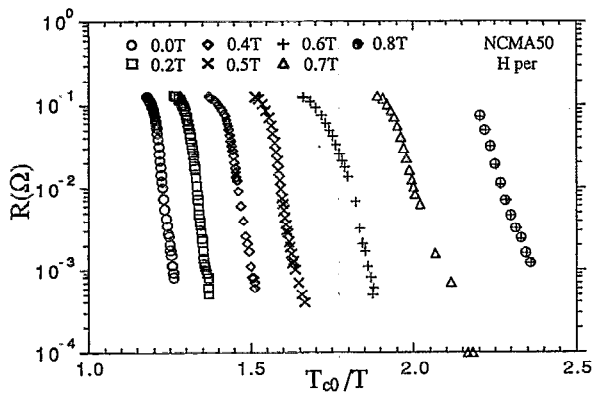


FIG. 7. Arrhenius plot of the $R(T)$ of the sample with 49.8 \AA of Cu(86)Mn(14) for different values of perpendicular magnetic field.

each multilayer normalized to the number of layers is equal to the resistance of a single layer. Below T^* the resistance has a higher thermally activation energy. Hence, a crossover was supposed from a regime where the vortex motion in a given layer is coupled, via a Josephson-like interaction, to the vortex motion in other layers ($T < T^*$), to a regime where the vortices, due to thermal fluctuations, display no interlayer coupling ($T > T^*$).

Our data, even though related to a SNS-like coupling in the presence of magnetic impurities, strongly support this model. In fact, we observed a crossover temperature T^* only in Nb-Cu(86)Mn(14) multilayers with thicknesses below 32 \AA . At larger thicknesses the Nb layers are completely decoupled at every temperature and the vortices cannot interact between layers. On the other hand, the fact we did not observe any crossover temperature T^* for Nb-Cu multilayers with Cu thicknesses up to 10 \AA could be also explained in terms of a stronger coupling between layers due to the weaker pair breaking mechanism.

Moreover, as shown in Fig. 8, the relation $T^*(H)/T_c^{\text{onset}}(H)$ decreases with increasing fields, so that the interlayer coupled vortex motion occurs increasingly far

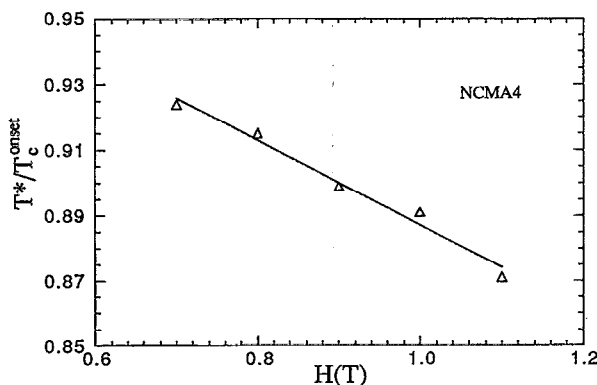


FIG. 8. The relation T^*/T_c^{onset} vs magnetic field. T^* corresponds to the temperature of the sharp downward kink.

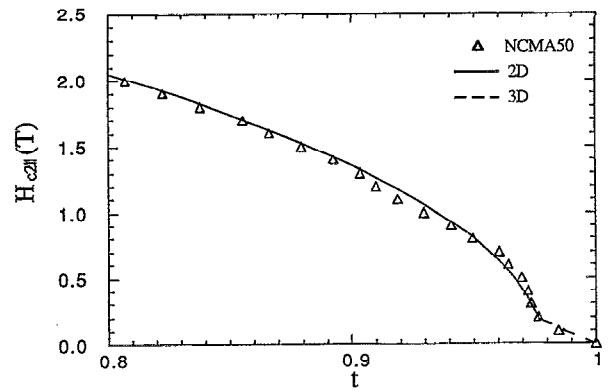


FIG. 9. Parallel critical magnetic field as a function of the reduced temperature for the sample of Fig. 7. The solid line corresponds to the 2D behavior, i.e., $H_{c2||} \sim (1-t)^{1/2}$. The dashed line is the best fit in the 3D case.

from T_c^{onset} at higher fields, confirming a vortex reconnection or related picture in which the important scale of vortex motion is the distance between them.

b. Parallel magnetic measurements. In Fig. 9 is shown the parallel critical magnetic field versus temperature curve for the sample of the series Nb-Cu(86)Mn(14) with $d_{\text{CuMn}} = 50 \text{ \AA}$. Close to T_c , the $H_{c2||}(T)$ curve behaves linearly while at lower temperatures the behavior is no longer linear, starting to be square-root-like as indicated by the solid line (square-root fit) and by the dashed line (linear fit). This effect has been already seen in many different superconducting multilayers, and it is essentially related to a 3D-2D crossover due to the layering and to the temperature dependence of the perpendicular superconducting coherence length $\xi_{\perp}(T)$ present in the equation for $H_{c2||}(T)$,²⁶

$$H_{c2||}(T) = \frac{\phi_0}{2\pi\xi_{\perp}(T)\xi_{||}(T)}. \quad (5)$$

According to the theoretical model of Josephson-coupled layered superconductors,²⁸ the jump in $H_{c2||}$ should happen when $\xi_{\perp}(T)/d_n \sim 0.7$. In our samples we always observed this jump to happen for $\xi_{\perp}(T)/d_n$ values higher than 1. This can be related to the different coupling mechanism between layers or to surface effects influencing the values of $\xi_{\perp}(T)$ calculated from the $H_{c2||}/H_{c2\perp}$ ratio. In fact, for samples of the series with Cu(86)Mn(14) we obtained $H_{c2||}/H_{c2\perp}$ values of 1.7 for thicknesses smaller than 16 \AA , indicating that the measured $H_{c2||}$ corresponds to H_{c3} . At larger thicknesses the $H_{c2||}/H_{c2\perp}$ ratio increases, giving increasing values of the Ginzburg-Landau mass ratio.²⁵

On the other hand, it seems difficult to ascribe the effect seen in the $H_{c2||}$ vs T curves to something related to magnetic phase ordering. Moreover, we did not observe any crossover of $H_{c2||}$ and $H_{c2\perp}$ near T_c , as foreseen in the case of the presence of magnetism in the spacer layer.²⁹ The same kind of measurements made on samples of the series with Cu(93)Mn(7) did not show any sign of this jump. The freezing temperatures of a multilayer of this series should be lower than that of the sample with equal CuMn thickness of the series with Cu(86)Mn(14) , so that if the jump were re-

lated to spin-glass ordering at $T \leq T_c$ it should be more clearly present in the curves of the lower Mn concentration samples. The Ginzburg–Landau mass ratio values for the series with Cu(93)Mn(7) are lower than those of the more magnetic series, and this is again an indication of the dimensional character of the effect.

III. CONCLUSIONS

We have fabricated spin-glass superconducting multilayers of Nb and CuMn. The decrease of T_c with the increasing of the CuMn layer thicknesses can be qualitatively explained in terms of models that take into account the possibility that the superconducting order parameter changes its phase in the range $0 \leq \phi \leq \pi$ when going from one superconducting layer to another.

The magnetic measurements with the external field in the direction perpendicular to the plane of the film have allowed us to study the behavior of the electronic diffusion coefficient of our multilayers and have shown at temperatures below T_c a crossover between two different kinds of vortex motion which was already observed in superconductor-insulator-superconductor multilayers and in high- T_c compounds.

When the magnetic field was applied parallel to the plane of the film, the measurements in the series with higher Mn concentration have shown the typical 3D-2D crossover related to the temperature dependence of $\xi_{\perp}(T)$.

ACKNOWLEDGMENT

This research has been supported in part by the U.S. Office of Naval Research under Contract No. N0014-92-J-1159.

- ¹F. Steglich, J. Aarts, C. D. Bredl, W. Lieke, D. Meschede, W. Franz, and H. Schafer, *Phys. Rev. Lett.* **43**, 1982 (1979).
- ²R. Chevrel, M. Sergent, and J. Prigent, *J. Solid State Chem.* **3**, 515 (1971).
- ³See *Superconductivity in Ternary Compounds II*, edited by M. B. Maple and O. Fisher (Springer, Berlin, 1982).
- ⁴R. Vaglio, B. D. Terris, J. F. Zasadzinski, and K. E. Gray, *Phys. Rev. Lett.* **53**, 1489 (1984).

- ⁵W. A. Fertig, D. C. Johnston, L. E. DeLong, R. E. McCallum, M. B. Maple, and B. T. Matthias, *Phys. Rev. Lett.* **38**, 987 (1977).
- ⁶D. Huser, M. J. F. M. Rewiersma, J. A. Mydosh, and G. J. Nieuwenhuys, *Phys. Rev. Lett.* **51**, 1290 (1983).
- ⁷S. Katano, T. Matsumoto, A. Matsushita, T. Hatano, and S. Funahashi, *Phys. Rev. B* **41**, 2009 (1990).
- ⁸M. L. Wilson, R. Loloee, and J. A. Cowen, *Physica B* **165-166**, 457 (1990).
- ⁹W. R. White, A. Kapitulnik, and M. R. Beasley, *Phys. Rev. Lett.* **66**, 2826 (1991).
- ¹⁰G. G. Kenning, J. M. Slaughter, and J. A. Cowen, *Phys. Rev. Lett.* **59**, 2596 (1987).
- ¹¹L. Hoines, R. Stubi, R. Loloee, J. A. Cowen, and J. Bass, *Phys. Rev. Lett.* **66**, 1224 (1991).
- ¹²G. G. Kenning, D. Chu, B. Alavi, J. M. Hammann, and R. Orbach, *J. Appl. Phys.* **69**, 5240 (1991).
- ¹³I. Banerjee, Q. S. Yang, C. M. Falco, and I. K. Schuller, *Solid State Commun.* **41**, 805 (1982).
- ¹⁴C. S. L. Chun, G. G. Zheng, J. L. Vicent, and I. K. Schuller, *Phys. Rev. B* **29**, 4915 (1984).
- ¹⁵L. Maritato, C. M. Falco, J. Aboaf, and D. I. Paul, *J. Appl. Phys.* **61**, 1588 (1987).
- ¹⁶M. Gurvitch, *Phys. Rev. B* **34**, 540 (1986).
- ¹⁷G. G. Kenning, J. Bass, W. P. Pratt, D. Leslie-Pelecky, L. Hoines, W. Leach, M. L. Wilson, R. Stubi, and J. A. Cowen, *Phys. Rev. B* **42**, 2393 (1990).
- ¹⁸P. G. de Gennes and E. Guyon, *Phys. Lett.* **3**, 168 (1963).
- ¹⁹N. R. Werthamer, *Phys. Rev.* **132**, 2440 (1963).
- ²⁰J. J. Hauser, C. Theurer, and N. R. Werthamer, *Phys. Rev.* **142**, 118 (1966).
- ²¹H. K. Wong, B. Y. Jin, H. Q. Yang, J. B. Ketterson, and J. E. Hilliard, *J. Low Temp. Phys.* **63**, 307 (1986).
- ²²L. N. Bulaeviskii, V. V. Kuzii, and A. A. Sobyenin, *JETP Lett.* **25**, 290 (1977).
- ²³Z. Radovic, M. Ledvij, L. Dobrosavljevic-Grujic, A. I. Buzdin, and J. R. Clem, *Phys. Rev. B* **44**, 759 (1991).
- ²⁴W. Stephan and J. P. Carbotte, *Phys. Rev. B* **46**, 317 (1992).
- ²⁵T. T. M. Palstra, B. Batlogg, R. B. Van Dover, L. F. Schneemeyer, and J. V. Waszczak, *Phys. Rev. B* **41**, 6621 (1990).
- ²⁶W. E. Lawrence and S. Doniach, in *Proceedings of the 12th International Conference on Low Temperature Physics*, Kyoto, Japan, 1970, edited by E. Kanda (Keigaku, Tokyo, 1971), p. 361.
- ²⁷J. Guimpel, M. E. de la Cruz, F. de la Cruz, H. J. Fink, O. Laborde, and J. C. Villegier, *J. Low Temp. Phys.* **63**, 151 (1986).
- ²⁸R. A. Klemm, M. R. Beasley, and A. Luther, *J. Low Temp. Phys.* **16**, 607 (1974).
- ²⁹S. Takahashi and M. Tachiki, *Phys. Rev. B* **33**, 4620 (1986).